Scientific Research and Essays Vol. 7(8), pp. 947-956, 29 February, 2012
Available online at http://www.academicjournals.org/SRE
DOI: 10.5897/SRE11.1909
ISSN 1992-2248 ©2012 Academic Journals

Full Length Research Paper

Friction stir spot welding parameters for polypropylene sheets

Memduh Kurtulmus

Department of Materials Technology, Marmara University, Istanbul, 34722, Turkey. E-mail: memduhk@marmara.edu.tr. Fax: +90 216 337 89 87.

Accepted 10 February, 2012

The friction stir spot welding (FSSW) method has four welding parameters: the welding tool rotational speed, tool plunge rate, tool plunge depth, the dwell time and tool retract delay. The effects of these welding parameters on joint formation and weld strength of polypropylene friction stir spot of welds were investigated. The effects of welding parameters on welding joint formation were determined by metallographic studies. The strength of welds were determined by the lap-shear test. From the experiments, it was found that the tool plunge rate had no effect on FSSW of polypropylene sheets. The effects of other important welding parameters were clearly discovered.

Key words: Polymer welding, friction stir spot welding, polymer friction stir spot welding, polypropylene welding.

INTRODUCTION

Spot welding is a very common joining technique in the automotive industry (Aslanlar et al., 2008). This welding process is widely used in the joining of sheet metal assemblies due to its advantages on welding efficiency and its suitability for automation (Goodarzi et al., 2008). Global trends force the automotive industry to manufacture lighter, safer, more environmentally friendly and ultimately cheaper vehicles (Blawert et al., 2004). Reduction in vehicle weight can be obtained by replacing conventional steels and cast irons with advanced high strength steels and light weight materials, such as aluminium, magnesium and reinforced polymer composites (Davies, 2003). These new automotive materials, however, have limited weldability characteristics which require improvements both in conventional welding processes and new welding techniques (Matsuyama, 2006).

In 2001, friction stir spot welding (FSSW) was developed in the automotive industry to replace resistance spot welding for aluminium sheets (Lin et al., 2008). The FSSW process consists of three phases; plunging, stirring and retracting as shown in Figure 1 (Lin et al., 2008). The process starts with the spinning of the tool at a high rotational speed. Then the tool is forced into the workpiece until the shoulder of the tool plunges into the upper workpiece. The plunge movement of the tool causes material to expel as shown in Figures 1a and b. When the tool reaches the predetermined depth, the plunge motion ends and the stirring phase starts. In this phase, the tool rotates in the workpieces without plunging. Frictional heat is generated in the plunging and the stirring phase and, thus, the material adjacent to the tool is heated and softened. The softened upper and lower workpiece materials mix together in the stirring phase. The shoulder of the tool creates a compressional stress on the softened material. A solid-state joint is formed in the stirring phase. When a predetermined bonding is obtained, the process stops and the tool is retracted from the workpieces. The resulting weld has a characteristic keyhole in the middle of the joint as shown in Figure 1c.

FSSW has been succesfully applied to aluminium (Merzoug et al., 2010), magnesium (Chen and Nakata, 2009) and steel (Khan et al., 2007) sheets, but there are very few publications on polymer FSSW applications (Gan et al., 2010; Arici and Mert, 2008; Oliviera et al., 2010; Filho et al., 2011; Bilici et al., 2010). Thus, this study was intended to explain the FSSW properties of polypropylene sheets. FSSW parameters such as the tool rotation speed, the plunge rate, the plunge depth and the dwell time are found to affect the FSSW nugget formation and the weld strength in metals (Santella et al., 2006).

Based on the observations of the FSSW macro-structures, the weld zone of a FSSW joint is schematically

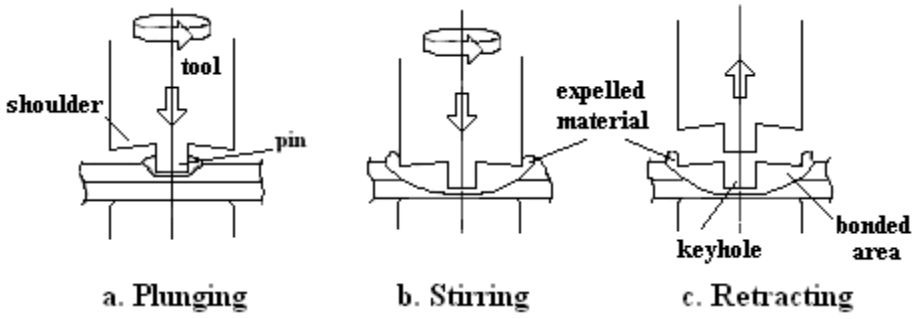

Figure 1. Three phases of friction stir spot welding process. (a), Plunging; (b), stirring; (c), retracting (Lin et al., 2008).

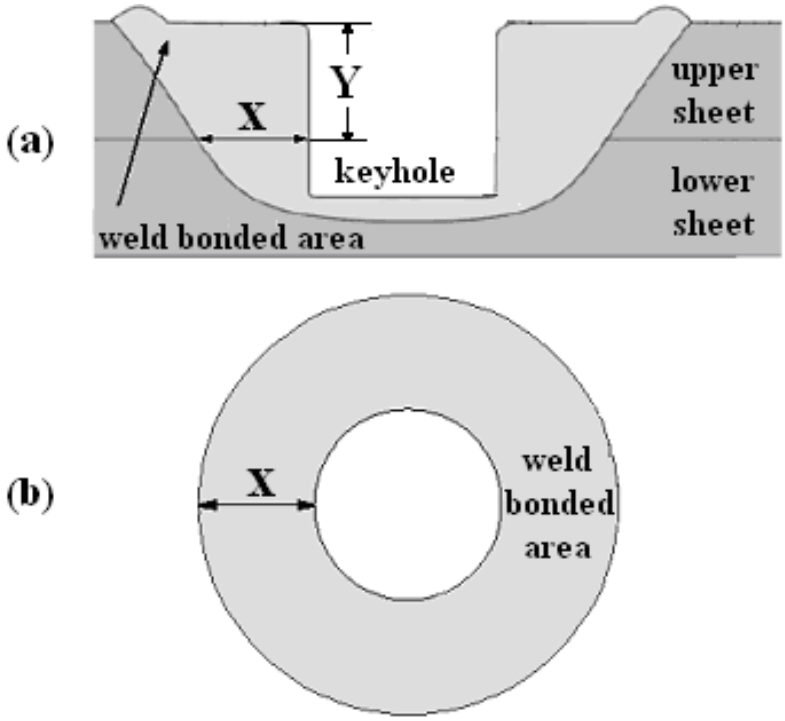

Figure 2. (a), Schematic illustration of the cross section of a friction stir spot weld; (b), geometry of the weld bond area (Gerlich et al., 2007); X, nugget thickness; Y, the thickness of the upper sheet.

shown in Figure 2 (Gerlich et al., 2007). From the appearance of the weld cross section, two particular points can be identified (Tozaki et al., 2007; Tozaki et al., 2007; Badarinarayan et al., 2007). The first point is the thickness of the weld nugget (x) which is an indicator of the weld bond area (Figure 2b). The weld bond area increases with the nugget thickness. The second point is the thickness of the upper sheet under the shoulder indentation (y). The size of these mentioned points determine the strength of a FSSW joint (Tozaki et al., 2007; Badarinarayan et al., 2007). There are numerous papers concerning the FSSW parameters which affect the joint geometry and the weld strength (Tozaki et al., 2007; Yang et. al., 2010; Karthikeyan and Balasubramanian, 2010; Tran et al., 2009).

MATERIALS AND METHODS

In this investigation, 4 mm thick polypropylene sheets were used. Figure 3 shows a lap-shear specimen used to investigate the FSSW under shear loading conditions. The specimens were welded in a milling machine. A spot weld joint was obtained in the middle of the specimen. In order to develop the FSSW tests, a properly designed clamping fixture was utilized to fix the specimens. Figure 4 shows a magnified cross sectional view of the tool used in the welding.

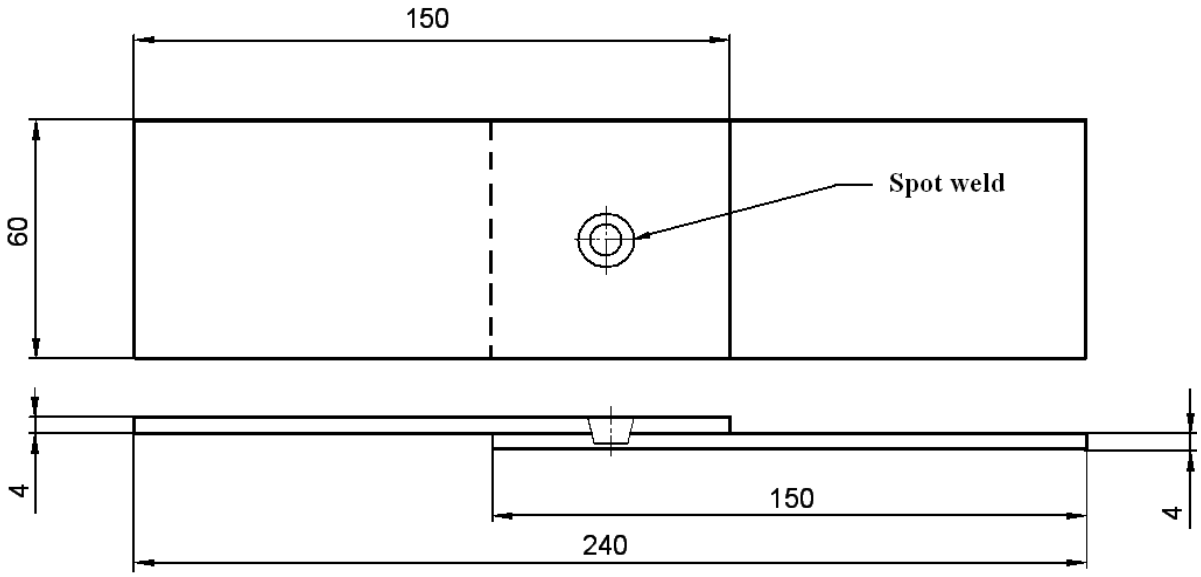

Figure 3. The size of a lap-shear test specimen.

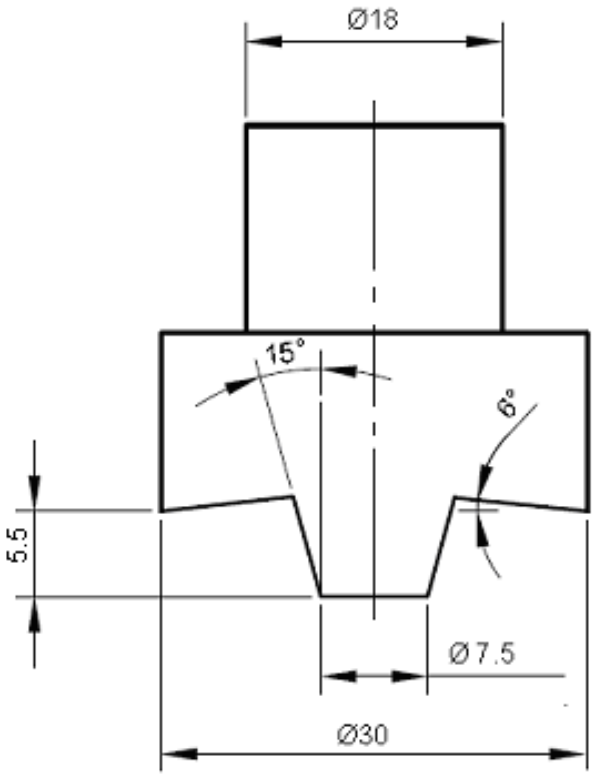

Figure 4. A magnified cross sectional view of the tool.

The tool was machined from SAE 1050 steel and heat treated to a hardness of 40 HRC. The rotating tool plunged into the workpieces with a certain plunge rate down to the required depth at an accuracy of ±0.02 mm. The stirring phase of the FSSW started with the completion of the tool plunging. In this phase, the tool rotated without plunging. The duration of this phase is called the dwell time. Upon reaching of the predetermined dwell time, the rotation of the tool was immediately stopped. All the welding

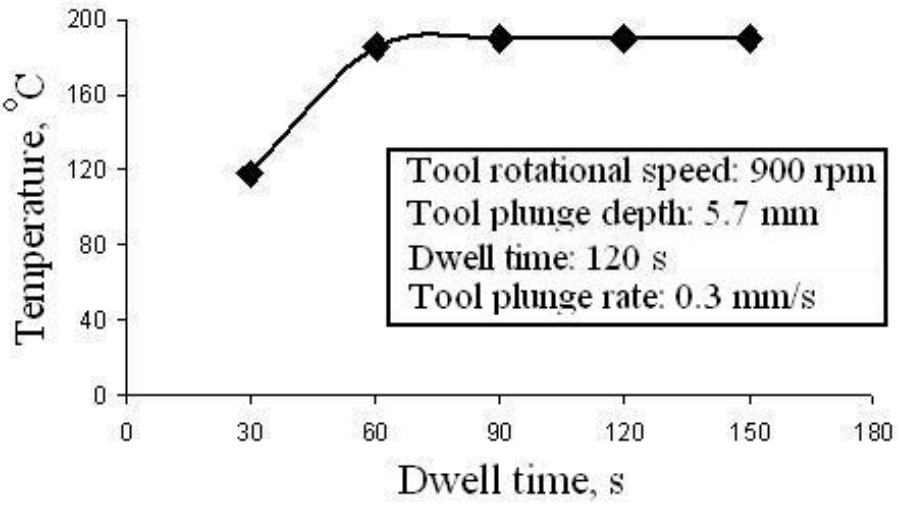

Figure 5. The effect of dwell time on weld zone temperature.

operations were done at the room temperature.

In temperature determining tests, the temperature of the weld joint was measured with an infrared thermometer. In a temperature measurement test, the tool was retracted immediately with the end of the dwell time and in other welding operations the tool stayed in the workpiece for 30 s with the end of the stirring phase and then it was retracted. In tool retract delay effect tests the tool waited 10 to 60 s in the weld zone after the end of the dwell time and then it was retracted. At each welding condition 6 lap-shear test specimens were produced. Five (5) of them were mechanically tested and the sixth one was metallographically examined.

Welded lap-shear specimens were tested on an Instron machine at a constant crosshead speed of 5 mm/s. The fracture load was recorded in the test. The lap-shear strength was obtained by averaging the strengths of 5 individual specimens, which were welded with identical welding parameters.

Weld cross section appearence observations of the joints were done with a video spectral comparator at 12.88X magnification. For macro structure studies, thin slices (30 µm) were cut from the welded specimens using a Leica R6125 model rotary type microtome. These thin slices were investigated using VSC-5000 model video spectral comparator. The photographs of the cross sections were obtained.

RESULTS

Temperature measurement and lap-shear test results were given graphically. In each graph, constant welding parameters were also indicated. The macrostructures of the welds are given behind the weld strength graphics. Thus, the effect of a welding parameter on joint formation and weld strength was clearly explained.

The effect of dwell time on the temperature of the weld zone is shown in Figure 5. The temperature in the weld zone increased with the duration of the dwell time. The temperature reached its maximum level (190°C) at 60 s. After 60 s, the temperature did not alter with the dwell time. The melting temparature of polypropylene is about 171°C (Mark, 1999). So the material of the weld zone was melted.

The effect of tool retracting delay on the weld cross section is shown in Figure 6. The cross section geometry of the weld joint depends upon the waiting time of the tool after the end of the dwell time. When the tool was immediately retracted, the joint did not show the characteristic keyhole (Figure 6 a). The joint that had a 30 s tool waiting time after the dwell time shows the characteristic keyhole (Figure 6b). The effect of tool delay time on weld strength is shown in Figure 7. The weld which did not have a tool retract delay has the lowest strength. The weld strength increased with the tool delay. Maximum weld strength was obtained with a 20 s tool delay. The delay time which is longer than 20 s has no effect on the weld strength.

Figure 8 shows the effect of dwell time on lap-shear tensile strength of FSSW joints. Increasing the dwell time from 30 to 60 s resulted in a linear progress in the strength of the welds. From 60 to 120 s of dwell time, there was a slight increase in the weld strength. The maximum tensile force was obtained with the 120 s dwell time. The weld strength decreased with the dwell time which is longer than 120 s. The effect of the dwell time on weld cross sections is shown in Figure 9. The nugget thickness increased with the dwell time. There is not a distinguished difference in the upper sheet thickness of the joints.

Figure 10 shows the effect of tool rotational speed on the weld strength. Only the tool rotational speed was allowed to vary in these experiments. The lowest strength was obtained at the 650 rpm speed. At this speed, a weak joint was obtained. The strength of the joint increased with the tool rotational speed. The peak strength was obtained at the 900 rpm speed. The weld strength decreased slightly with increase in the rotational

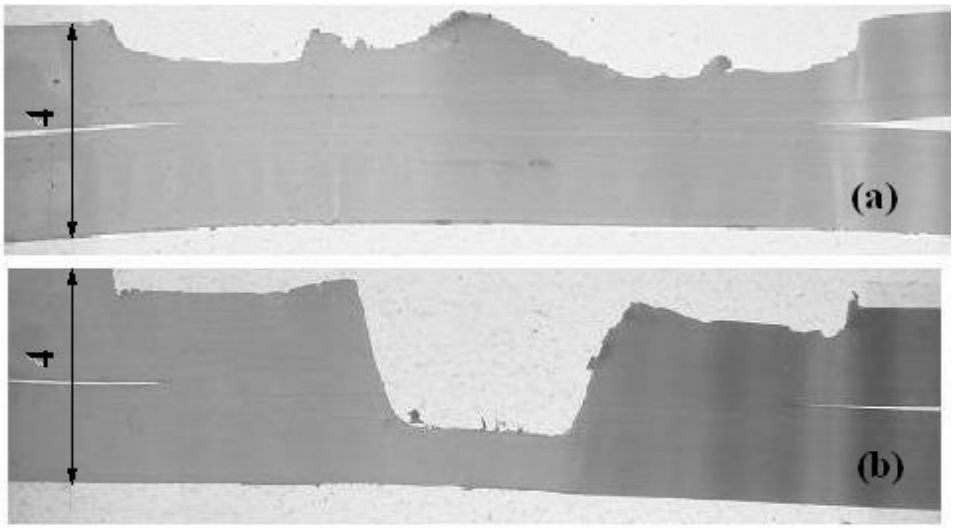

Figure 6. The effect of tool retracting delay on weld cross section. (a), No delay; (b), 30 s delay.

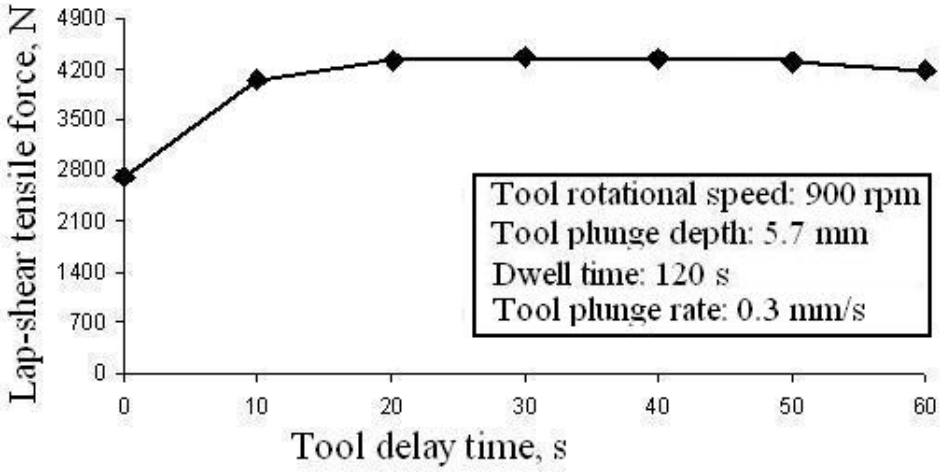

Figure 7. The effect of tool delay time on weld strength.

speed beyond the 900 rpm tool rotational speed. The effect of tool rotational speed on weld joint is shown in Figure 11. In these joints, only nugget thickness varied. The thickness increased with the tool rotational speed.

Figure 12 shows the effect of the tool plunge depth on the strength of the joints. In these tests only plunge depth varied between 5.6 to 7.0 mm. At the 5.6 mm plunge depth, a low strength was obtained. The strength of the joint increased with the plunge depth. The maximum strength was obtained at the 5.7 mm plunge depth. The strength of the joint decreased with increase in the plunge depth more than 5.7 mm. The effect of the plunge depth on the joint cross section is shown in Figure 13. In these weld nugget thickness increased and the upper sheet thickness dicreased with the plunge depth. The minimum upper sheet thickness and maximum nugget thickness was obtained with the 7.0 mm tool plunge depth.

Figure 14 shows the effect of the plunge rate on the strength of joints. Figure 14 shows that the tool plunge rate has a negligible effect on FSSW of polypropylene sheets. Although, the plunge rate was increased up to twelve folds, the weld strength changed only within experimental scatter limits.

DISCUSSION

Figure 5 shows the effect of the dwell time on the temperature of the weld zone material. The temperature

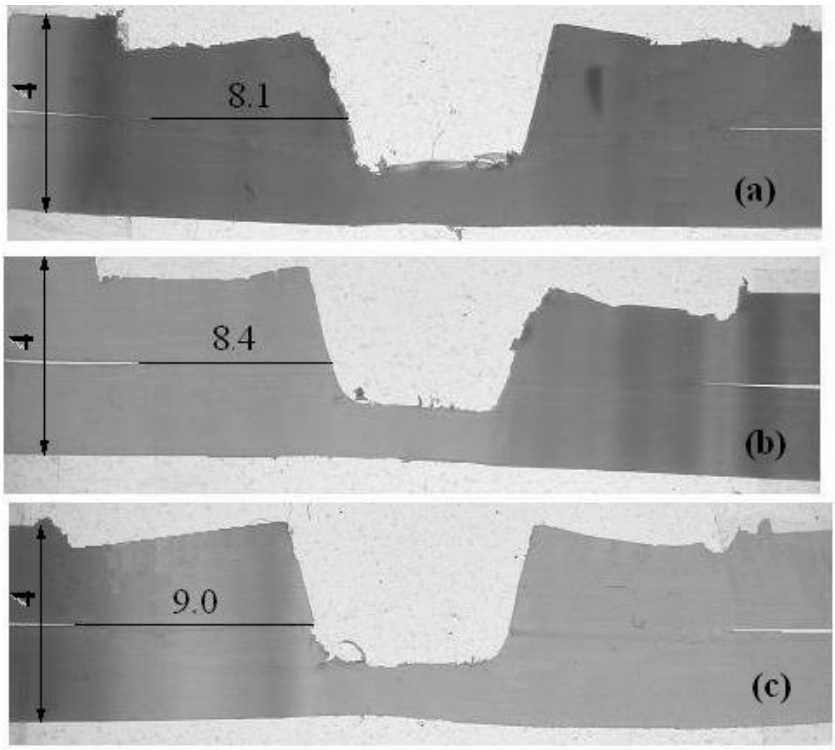

Figure 9. The effect of the dwell time on the joint cross section: (a), 60 s dwell time; (b), 120 s dwell time; (c), 240 s dwell time.

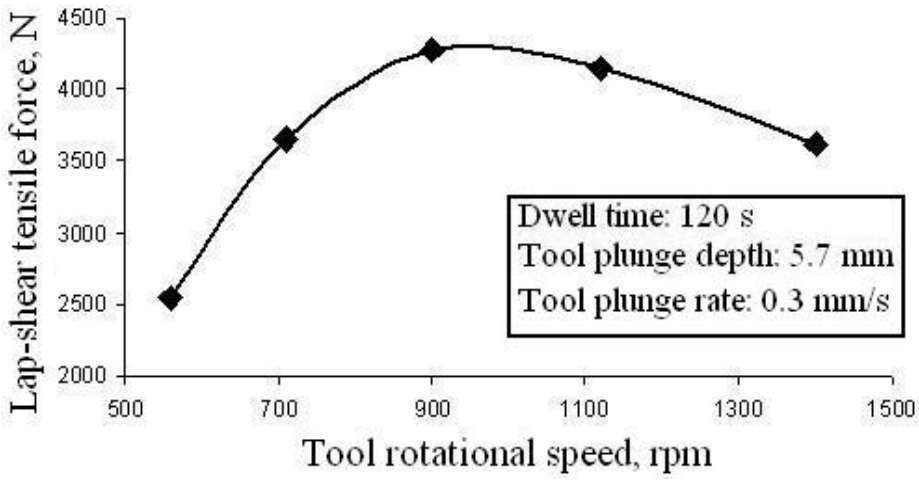

Figure 10. The effect of tool rotational speed on lap-shear tensile fracture load.

of the material increased with the dwell time. The friction heat produced in the vicinity of the tool increased with the dwell time (Ma et al., 2009), so the temperature of the material increased as shown Figure 5. The temperature of the material reached the melting temperature (171°C) with a 50 s dwell time. The temperature rose up to 190°C with 60 s dwell time and it did not change with extended dwell time. Similar over melting temperatures were calculated in friction stir welding of HDPE sheets (Bilici et al., 2011; Aydın, 2010). If the tool retracted with the end of the predetermined dwell time, the liquid filled the space of the pin as shown in Figure 6a. If the pin retracted with 30 s delay, the liquid in the vicinity of the pin cooled and solidified with the keyhole as shown in Figure 6b. The

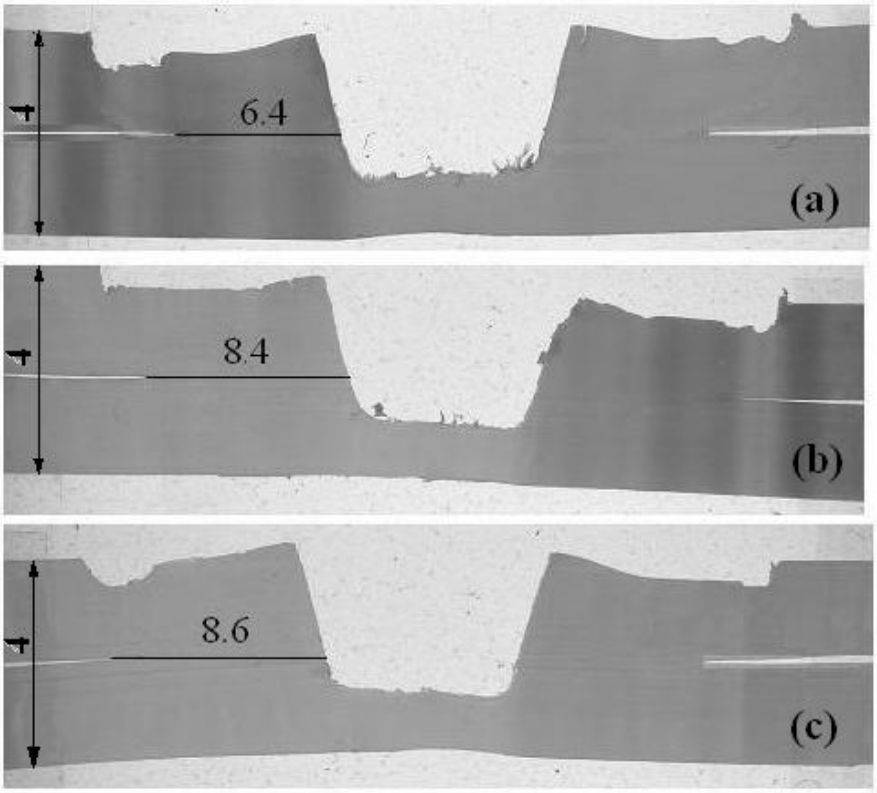

Figure 11. The effect of the tool rotational speed on the joint cross section. (a), 710 rpm tool rotational speed; (b), 900 rpm tool rotational speed; (c), 1100 rpm tool rotational speed.

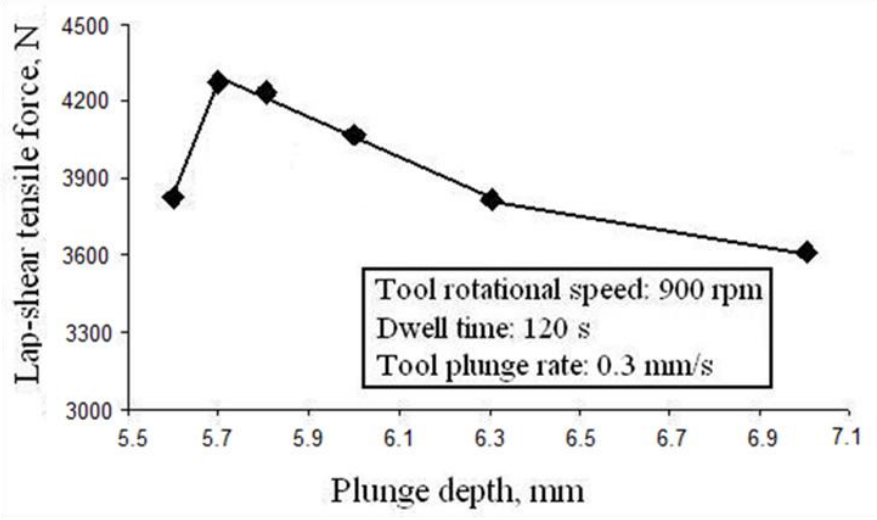

Figure 12. The effect of tool plunge depth on lap-shear tensile fracture load.

tool delay time also affects the weld strength as shown in Figure 7. At least 20 s delay time is needed to obtain a high weld strength. This 20 s delay time is necessary to solidify the liquid weld zone material. In this period, heat transfers from the liquid to the steel welding tool and the characteristic keyhole forms in the weld zone. Figures 5 and 6 clearly show that polypropylene FSSW is not a solid-state joining method. During the welding operation,

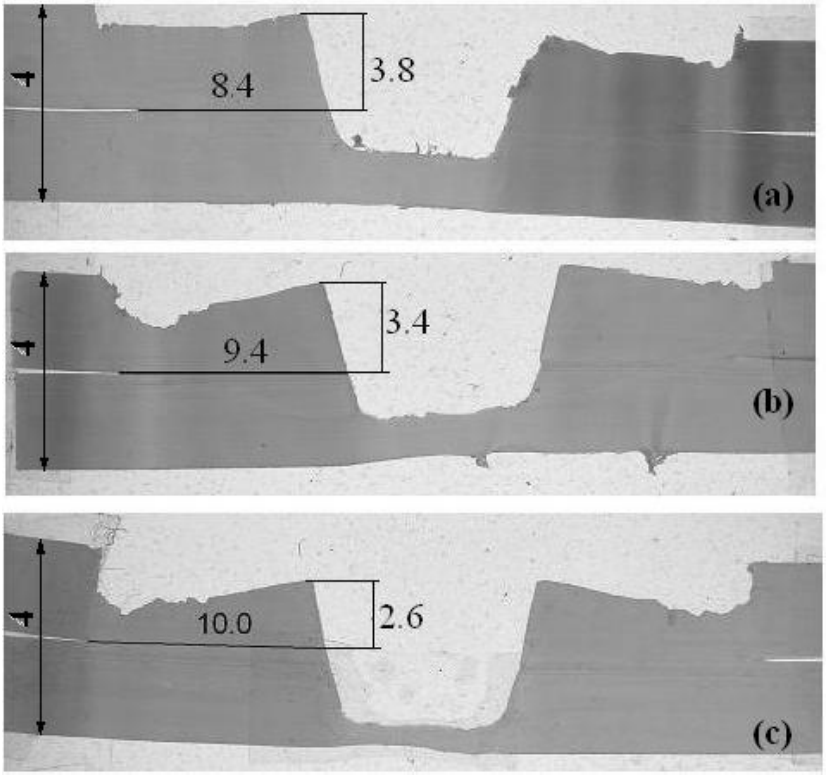

Figure 13. The effect of plunge depth on joint cross section. (a), 5.7 mm plunge depth; (b), 6.3 mm plunge depth; (c), 7.0 plunge depth.

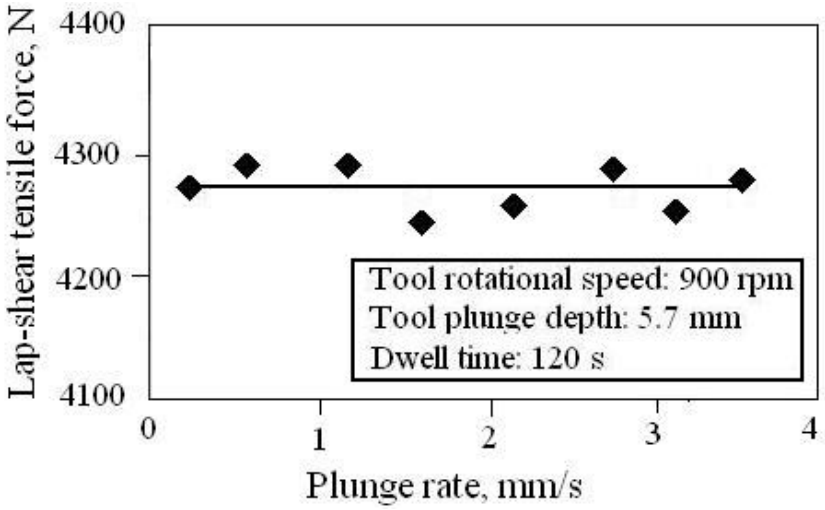

Figure 14. The effect of tool plunge rate on lap-shear tensile fracture load.

the material around the tool melts, joins in the liquid state and then it solidifies.

The dwell time is very important in FSSW of metals (Merzoug et al., 2010). The friction heat increases with the dwell time (Awang et al., 2005). The amount of friction heat produced in the weld area determines the size of the joint. A big weld bond area is produced with a high friction heat (Ma et al., 2009). Figure 9 shows the effect of dwell time on the joint cross section. The thickness of the upper sheet did not alter with the dwell time but the nugget thickness increased with the dwell time. The nugget thickness was 8.1 mm for the 60 s

dwell time and it enlarged to 9.0 mm for the 240 s dwell time. There is a direct relationship between the nugget thickness and the weld bond area (Tozaki et al., 2007). The weld bond area determines the strength of a weld in metals (Gerlich et al., 2007). The joint strength increases with the weld bond area (Santella et al., 2006). Figure 8 shows the effect of dwell time on lap-shear fracture load. A very weak weld strength was obtained with the 30 s dwell time. The nugget thickness of this weld was about 2.0 mm. The very small bond area of this weld caused a very low fracture load. The strength of the weld increased with the dwell time as shown in Figure 8. The increase in the joint strength was due to the increase of the weld bond area (Figure 9). The maximum weld strength was obtained with 120 s dwell time. When the dwell time exceeded 120 s the weld strength decreased. For example, only 3400 N weld fracture load was obtained with the 240 s dwell time. Although this weld had a thicker nugget than the 120 s weld (Figure 9), its fracture load was 880 N less than the other. The reason of this strength difference is due to the mechanical scission (Costa et al., 2005). Mechanical scission lowers the strength of a thermoplastic material (Capone et al., 2007). If a thermoplastic material is heated to a high temperature and then a high pressure is applied to it, a decrease in the molecular weight of the material occurs. The mechanical properties of thermoplastics decrease with lowering the molecular weight (Lim et al., 2004). In FSSW, the welding tool produces a compressive pressure in the weld zone (Gerlich et al., 2007). The material in the weld area is liquid in polypropylene FSSW as explained earlier. In this study, only the outer temperature of the weld area was measured. In these tests not very high temperatures were measured. But some authors measured very high temperatures in the vicinity of the tool pin (Oliveria et al., 2010; Aydin., 2010). A high material temperature and a high tool pressure caused mechanical scission in thermoplastic friction stir welding (Bozzia et al., 2010). A smilar mechanical scission occurred in polypropylene FSSW which lowered the weld strength as shown in Figure 8.

Figure 10 shows the effect of tool rotational speed on the weld strength. The lowest strength was obtained at the 560 rpm tool rotational speed. The weld strength increased with the rotational speed from 560 to 900 rpm. Figure 11 shows the effect of the tool rotational speed on weld cross section. The friction heat produced in the weld zone increased with the rotational speed. The high friction heat affects the nugget formation. The tool speed has a negligible effect on the thickness of the upper sheet. It has an important effect on the weld nugget thickness. The nugget gets thicker with the tool rotational speed. Optimum weld strength was obtained with the 900 rpm tool speed. The weld strength decreased with increasing the tool speed over 900 rpm. There are two reasons to explain the decrease of the weld strength.

One of them is the mechanical scission which was already explained earlier. The second reason is the residual stresses of the welding procedure. Residual stresses are being created in FSSW joints (Bozzia et al., 2010). Especially the residual stress of the upper sheet was important for the weld strength. The residual stresses decrease the load carrying capacity of the weld (Bozzia et al., 2010). The residual stress of the upper sheet increases with rotational speed which result as a low strength. The stirring effect of the pin increases with the tool rotational speed (Ma et al., 2009). High residual stresses decrease the weld strength.

Figure 12 shows the effect of the tool plunge depth on the strength of the FSSW joints. At the 5.6 mm plunge depth, a low weld strength was obtained. The weld strength increased with the plunge depth. The maximum weld strength was obtained at the 5.7 mm plunge depth. Then the joint strength decreased with the plunge depth. The effect of plunge depth on weld nugget formation is shown in Figure 13. The inner diameter of the keyhole increased with the plunge depth because a tapered cylindrical pin tool was used in welding. The weld thickness increased but the thickness of the upper sheet decreased with the plunge depth. The pressure of the tool increased with the tool plunge depth (Ma et al., 2009). The friction heat produced in the weld area increased with the tool pressure (Awang et al., 2005) and thicker weld nuggets were obained. A big weld bond area can increase the weld strength of the joint but two contrary factors decrease the weld strength. The effective contrary factors are the mechanical scission and the small upper sheet thickness. High tool pressures provoke mechanical scission. The other factor is thinning of the upper sheet thickness with the plunge depth. The weld strength decreases with thinning the upper sheet thickness (Tozaki et al., 2007; Badarinarayan et al., 2007). These two negative factors lowered the weld strength beyond the 5.7 mm plunge depth.

Conclusions

From this study the following results were obtained:

1) The dwell time, tool otational speed and the plunge depth affect the FSSW nugget formation and the strength of the joint. Optimum parameters must be used to obtain high quality welds. In the study, 900 rpm tool rotational speed, 120 s dwell time and 5.7 mm plunge depth was determined as the optimal welding parameters.
2) The plunge rate of the tool has a negligible effect on the polypropylene FSSW joint strength.
3) Melting of polypropylene occurred in the vicinity of the tool pin.
4) Mechanical scission occurs in polypropylene FSSW.

REFERENCES

Arici A, Mert S (2008). Friction stir spot welding of polypropylene, J.

Reinforced Plast. Compos., 1: 1-4.
Aslanlar S, Ogur A, Ozsarac U, Ilhan E (2008). Welding time effect on mechanical properties of automotive sheets in electrical resistance spot welding. Mater. Des., 29: 1427-1431.
Awang M, Mucino VH, Feng Z, David SA (2005). Thermo-mechanical modeling of friction stir spot welding (FSSW) process: Use of an explicit adaptive meshing scheme. SAE Technical Paper No:01-1251, Society of Automotive Engineers, Warrendale, PA.
Aydin M (2010). Effects of Welding Parameters and Pre-Heating on the friction stir welding of UHMW-polyethylene. Polym. Plast. Technol. Eng., 49: 595-601.
Badarinarayan H, Shi Y, Li X, Okamoto K (2007). Effect of tool geometry on hook formation and static strength of friction stir spot welded aluminum 5754-O sheets. Int. J. Machine Tools Manuf., 49(11): 814-823.
Bilici MK, Yükler AI, Kurtulmus M (2011). The optimization of welding parameters for friction stir spot welding of high density polyethylene sheets. Mater Des., 32(7): 4074-4079.
Blawert C, Hort N, Kainer KV (2004). Automotive applications of magnesium and its alloys. Trans. Indian Instit. Metals., 57: 397-408.
Bozzi S, Helbert AL, Baudin T, Klosek V, Kerbiguet JG, Criqui B (2010). Influence of FSSW parameters on fracture mechanisms of 5182 aluminium welds. J. Mater. Process. Technol., 210: 1429-1435.
Capone C, Landro LD, Inzoli F, Penco M, Sartore L. (2007). Thermal and mechanical degradation during polymer extrusion processing. Polym. Eng. Sci., 47: 1813- 1819.
Chen YC, Nakata K (2009). Effect of tool geometry on microstructure and mechanical properties of friction stir lap welded magnesium alloy and steel. Mater Des., 30: 3913- 3919.
Costa HM, Ramos VD, Rocha MCG (2005). Rheological properties polypropylene during multiple extrusion. Polym. Test., 24: 86-93
Davies G (2003). Future trends in automotive body materials. Mater. Autom. Bodies., 8: 252-269
Gan YX, Daniel S, Reinbolt M (2010). Friction Stir Processing of Particle Reinforced Composite Materials. Mater., 3: 329-350.
Gerlich A, North TH, Yamamoto M (2007). Local melting and cracking in Al 7075-T6 and Al 2024-T3 friction stir spot welds. Sci. Technol. Weld. Join., 12: 472-480.
Goodarzi M, Marashi SPH, Pouranvari M (2009). Dependence of overload performance on weld attributes for resistance spot welded galvanized low carbon steel. J. Mater. Proces. Technol., pp. 4379-4384.
Filho STA, Bueno C, Santos JF, Huber N, Hage E (2011). On the feasibility of friction spot joining in magnesium/fiber reinforced polymer composite hybrid structures. Mater. Sci. Eng. A., 528: 3841-3848.
Karthikeyan R, Balasubramanian V (2010). Predictions of the optimized friction stir spot welding process parameters for joining AA2024 aluminum alloy using RSM Int J. Adv. Manuf. Technol., (51): 173-183.
Khan MI, Kuntz ML, Su P, Gerlich A, North T, Zhou Y (2007). Resistance and friction stir spot welding of DP 600: A comparative study. Sci. Technol. Weld. Join., 12: 175-182.
Lim ST, Kim CA, Chung H, Choi HJ, Sung JH (2004). Mechanical degradation kinetics of polythelene oxide in a turbulent flow. Korea-Australia rheol. J., 2: 57-62.
Lin PC, Pan J, Pan T (2008). Failure modes and fatigue life estimations of spot friction welds in lap-shear specimens of aluminium 6111-T4 sheets. Part 2: Welds made by a flat tool. Int. J. Fatigue., 30: 90-105.
Ma N, Kunugia A, Hirashima T, Okubo K, Kamioka M (2009). FEM Simulation for friction spot joining process. Weld. Int., 23 (1): 9-14.
Mark JE (1999). Polymer Data Handbook, Oxford University Press, New York.
Matsuyama K (2006). Trend of automobile vehicles and the joining technologies. Int. Weld. Ins Doc IIW Doc III., 1386-06.
Merzoug M, Mazari M, Berrahal L, Imad A (2010). Parametric studies of the process of friction spot stir welding aluminium 6060-T5 Alloys. Mater. Des., 31: 3023-3028.
Oliveria PHF, Filho STA, Santos JF, Hage E (2010). Preliminary study on the feasibility of friction spot welding in PMMA . Mater. Lett., 64: 2098-2101.
Santella ML, Grant GJ, Feng Z, Hovanski Y (2006). Friction stir spot welding of advanced high strength steel. FY Progress Report, Oak Ridge National Laboratory.
Tozaki Y, Uematsu Y, Tokaji K (2007). Effect of processing parameters on static strength of dissimilar friction stir spot welds between different aluminium alloys. Fatigue Fracture Eng. Mater. Struct., 30: 143-148.
Tozaki Y, Uematsu Y, Tokaji K (2007). Effect of tool geometry on microstructure and Static strength in friction stir spot welded aluminium alloys Inter J. Mach. Tools Manuf.,47: 2230-2236.
Tran VX, Pan J, Pan T (2009). Effects of processing time on strengths and failure modes of dissimilar spot friction welds between aluminum 5754-O and 7075-T6 sheets. J Mater Process Technol., 8: 3724-3739
Yang Q, Mironov S, Sato YS, Okamoto K (2010). Material flow during friction stir spot welding. Mater. Sci. Eng. A., 527(16-17): 4389-4398.